Iğdır Üniversitesi Fen Bilimleri Enstitüsü Dergisi, 14(4), 1717-1730, 2024
Journal of the Institute of Science and Technology, 14(4), 1717-1730, 2024

ISSN: 2146-0574, eISSN: 2536-4618

Matematik / *Mathematics* **DOI: 10.21597/jist.1496717**

Araştırma Makalesi / *Research Article*

Geliş tarihi / *Received*: 06.06.2024 **Kabul tarihi / *Accepted*: 26.08.2023**

Atıf İçin: Karaagac, B., Esen, A. ve Uzunyol, M. H. (2024). Zaman kesirli Klein Gordon denklemine yeni sayısal bakış açısı. *Iğdır Üniversitesi Fen Bilimleri Enstitüsü Dergisi*, 14(4), 1717-1730.

To Cite: Karaagac, B., Esen, A. & Uzunyol, M. H. (2024). Numerical Solutions of Time fractional Klein Gordon Equation using Crank-Nicolson Finite Difference Method. *Journal of the Institute of Science and Technology*, 14(4), 1717-1730.

Zaman Kesirli Klein Gordon Denkleminin Crank-Nicolson Sonlu Farklar Yöntemi ile Sayısal Çözümleri

Berat KARAAGAC[1]*, Alaattin ESEN[2], Muhammed Huzeyfe UZUNYOL[2]

Öne Çıkanlar:

- Kesirli Türev
- Nümerik çözümler
- Von Neumann Kararlılık analizi

Anahtar Kelimeler:

- Kesirli Klein Gordon denklemi
- Sonlu Fark Yöntemleri
- Kararlılık Analizi

ÖZET:

Sonlu fark yöntemleri fen ve mühendislik gibi birçok alanda gözlemlenen kısmi diferansiyel denklemlerin çözümünde yaygın olarak kullanılan sayısal bir yöntemdir. Bu araştırma, kuantum alanlarındaki anormal difüzyonu ve dalga yayılımını tanımlayan ve Caputo anlamında zamana göre kesirli türeve sahip Klein Gordon denkleminin nümerik çözümleri hakkında bir inceleme sunmaktadır. Araştırmanın içeriğinde sonlu fark yöntemlerinin temel karakteristiklerini göz önüne alınarak ilk olarak problemin çalışıldığı bölge ayrıklaştırılır. Daha sonra, zamana göre türev $L2$ algoritması ve diğer terimler ise Crank-Nicolson sonlu fark yaklaşımı yardımıyla ayrıklaştırılarak bir cebirsel denklem sistemi elde edilir. Elde edilen Cebirsel denklem sisteminin çözülmesi ise nümerik çözümlerin üretilmesi ile sonuçlanır. Nümerik sonuçlar, denkleme ait parametrelerin ve kesirli mertebeden türevin α(1≤α≤2) çeşitli değerleri için hesaplanarak hata normları hesaplanır. Grafiksel bulgular ise kesirli mertebenin çeşitli değerleri için yaklaşık çözümlerin fiziksel davranışını sergilemektedir. Ayrıca, nümerik şemanın kararlılık analizi von-Neumann kararlılık analizi ile araştırılır. Bu çalışmanın sonuçları bu çalışmada sunulan yöntemi bu alanda çalışan diğer araştırmacıların doğadaki olayları modelleyen diğer problemlere uygulamalarına yardım edecektir.

Numerical Solutions of Time fractional Klein Gordon Equation using Crank-Nicolson Finite Difference Method

Highlights:

- Fractional derivative
- Numerical Solutions
- Von Neumann Stability analysis

Keywords:

- Fractional Klein Gordon equation
- finite difference technique
- Stability analysis

ABSTRACT:

Finite difference methods are widely used numerical techniques used to solve partial differential equations observed in many fields, such as science and engineering. This research presents a study on the numerical solutions of the Klein-Gordon equation, which describes anomalous diffusion and wave propagation in quantum fields and possesses a fractional derivative in the Caputo sense. The content of the paper begins by discretizing the region of the problem while taking into account the fundamental characteristics of finite difference methods. Subsequently, the time derivative $L2$ algorithm, and the other terms, are discretized using the Crank-Nicolson finite difference approach, resulting in a system of algebraic equations. Solving this algebraic equation system yields numerical solutions. The numerical results are calculated for various values of the parameters associated with the equation and fractional order derivatives α(1≤α≤2), leading to the computation of error norms. Graphical findings illustrate the physical behavior of approximation solutions for a variety of fraction order values. Additionally, the stability analysis of the numerical scheme is investigated using von-Neumann stability analysis. The results of this paper will help other researchers studying in the field to apply the presented method to other problems modelling the natural phenomena.

[1]Berat KARAAGAC (**Orcid ID:** 0000-0002-6020-3243), Adıyaman Üniversitesi, Eğitim Fakültesi, İlköğretim Matematik Öğretmenliği Bölümü, Adıyaman, Türkiye
[2]Alaattin ESEN (**Orcid ID:** 0000-0002-7927-5941), İnönü Üniversitesi, Fen Edebiyat Fakültesi, Matematik Bölümü, Malatya, Türkiye
[3]Muhammed Huzeyfe UZUNYOL (**Orcid ID:** 0009-0008-3723-6902), İnönü Üniversitesi, Fen Edebiyat Fakültesi, Matematik Bölümü, Malatya, Türkiye.

***Sorumlu Yazar/*Corresponding Author*:** Berat KARAAĞAÇ, e-mail: bkaraagac@adiyaman.edu.tr

INTRODUCTION

Fractional calculus has a history old and deep-rooted as classical calculus. It is a branch of mathematics that carries the traditional order of derivatives and integrals into an arbitrarily complex order. The history of fractional calculations are based on the work of mathematicians and scientists over several centuries, beginning with a question first raised by L'Hopital on September 30, 1695, about Leibniz's notation what the result would be if $n = 1/2$ at $D^n x / Dx^n$ (Paredes, 2020). However, the interest in this topic has begun to grow around 1890, leading to the definition of various operators as a result of the in-depth investigation of fractional calculus. Initially, the Riemann-Liouville derivative was introduced. Later, in 1967, Caputo fractional derivatives were introduced, which offer advantages in physical problems (Korichi et al., 2024). The Caputo fractional operator played a significant role in fractional calculus due to its ability to handle initial value problems and provide a more suitable framework for modeling real-world dynamical systems. Over time, numerous definitions, operators, models, and rules for evaluating fractional calculus operators emerged, driven by various considerations. The motivation behind of this topic is the need for applied scientists to develop models that accurately describe a wide range of systems and extend the field of fractional calculus. Building on this motivation, this paper aims to obtain numerical solutions of the Klein-Gordon equation defined with the Caputo sense fractional derivative with respect to time.
The equation is described along with its initial-boundary conditions as follows (Nagy, 2017):

$$D_t^{\alpha} u = u_{xx} + au + bu^2 + cu^3 + g(x,t) \tag{1}$$

$$\begin{aligned} &u(x_L,t) = u_L(t), \quad u(x_R,t) = u_R(t), \quad x_L \le x \le x_R \\ &u(x,0) = f_1(x), \quad u_t(x,0) = f_2(x), \quad 0 \le t \le T. \end{aligned} \tag{2}$$

To achieve our aim, we will use finite difference methods. In more detail, the $L2$ algorithm will be used to discretize the time fractional-order derivative. The spatial derivatives will first be discretized using the Crank-Nicolson approximation to contribute to the time progression and obtain more accurate results. Then, the difference approximations will be written in place of the terms containing derivatives using central difference approximations. For the purposes of this paper, we will investigate the dynamics of the fractional order Klein-Gordon equation applying the finite difference technique, the Crank-Nicolson approximation, the Rubin-Graves linearization, and the $L2$ algorithm. Furthermore, the techniques' application and how the error rate is impacted by space and time step size changes in as well as the stability analysis structure for fractional order equation classes, will be discussed. In addition, it is aimed to contribute to the literature by combining these three techniques and analyzing their effect on the solutions of a nonlinear partial differential equation. In addition, the examination of the fractional order Klein-Gordon equation with two sample problems will enable the evaluation of the method's accuracy. The last but not least, the numerical results will contribute to the phsical examination of the phenomena lying behind the handled equation.

The content of the present paper is as follows: In the next section, the aforementioned equation and notations used in the method will be introduced. In the following section, the application of the method to the time-fractional Klein-Gordon equation will be discussed, and then the stability analysis of the numerical scheme obtained in the previous section will be considered using the von Neumann method. In the final section, the numerical outcomes and error norms will be presented in tables and graphs, showcasing a visual representation of the equation's structure.

MATERIALS AND METHODS

Fractıonal Kleın Gordon Equatıon and Fınıte Dıfference Method

The time fractional Klein-Gordon (TFKG) equation is an extended version of the traditional Klein-Gordon equation as replacing the constant order fractional time derivative by fractional order time derivative. The time-fractional Klein-Gordon equation has a range of applications in theoretical physics, particularly in the paper of relativistic quantum mechanics, quantum field theory, and the behavior of quantum particles in non-local and non-integer order systems. Using this equation, researchers provide a more thorough framework for evaluating the dynamics of relativistic quantum fields, especially in cases where non-integer order behavior and long-range interactions are common. In Eq. (1), a,b, and c are real constants, u stands for an unknown function in the variables x and t. $D_t^{\alpha}(.)$ denotes fractional order derivative in Caputo sense and α is $1\leq\alpha\leq2$. $g(x,t)$ indicates the source term and $u_0(x)$, $u_L(t)$, $u_R(t)$ are given functions and $f_2(x)$ is initial velocity of the wave which is produced via the equation. In the literature, there have been a lot of valuable studies on time fractional Klein Gordon equation. Among others, some of these are; (Habjia et al.,2024) investigated space-time fractional Klein-Gordon equations and used the sine approach to generate accurate solutions. (Mirzaei & Shokri, 2024) have proposed a numerical approach to solve the nonlinear time fractional Klein-Gordon equation. They used a pseudo-spectral approach based on Lagrange polynomials at Chebyshev points to approximate spatial derivatives. (Odibat,2024) has developed a numerical method using finite difference methods and predictor-corrector methods to obtain numerical solutions to the investigated problems. (Vivas-Cortez et al., 2024) have used Extended cubic B-spline (ECBS) functions for obtaining the numerical solutions of the generalized nonlinear time-fractional Klein-Gordon equation (TFKGE). In (Sahu & Jena, 2024), a hybridized Newton-Raphson approach is used with a modified Laplace Adomian decomposition technique (LADT) to investigate an approximate solution to the Time Fractional Klein Gordon Equation (TFKGE). (Ganji et al., 2021) have described a novel approach that uses the clique polynomial as the basis function for the operational matrices to generate a time-FKGE solution. (Mohebbi et al., 2014) have used a high-order difference approach to solve some time-fractional PDEs including Cattaneo equation, linear time fractional and dissipative Klein-Gordon equations. (Nagy, 2017) has used an accurate numerical approach, which depends on the Sinc function and second-order shifted Chebyshev polynomials, to solve the time fractional nonlinear Klein–Gordon equation. (Amin et al., 2020) have developed an extended cubic B-spline functions approach to investigate the approximate solution of the time-fractional Klein-Gordon problem. In (Akram et al., 2020), authors have used a new extended cubic B-spline (ECBS) approximation to numerically solve the equation. (Mulimani & Kumbinarasaiah, 2024) have constructed a numerical technique using Fibonacci wavelets in order to solve fractional Klein-Gordan equations (FKGEs). Biswas (Biswas, 2024) has investigated the behavior of the Poschl-Teller potential in the D-dimensional Klein-Gordon equation, employing the Green-Aldrich technique. For more information, researchers can check the references given in (Odibat & Momani, 2009; Dehghan et al., 2015; Hashemizadeh & Ebrahimzadeh, 2018; Bansu & Kumar, 2021; Yaseen et al., 2021).

In order to explain finite difference notations, the spatial domain and time domain are choosen as $[x_L,x_R]$ and $[0,T]$, respectively. Now, we are going to begin by establishing N nodes of computational domain and M nodes of time domain such as $\{x_j\}\Big|_{x_L}^{x_R}$ where $\Delta x = x_{j+1}-x_j \ \ (j=0,1,..,N)$, $\{t_n\}\Big|_0^T$ where

$\Delta t = t_{n+1} - t_n \ \left(n = 0,1,2,..,M\right)$. Then, as procedure of finite difference method, the derivatives of function $u\left(x,t\right)$ will be replaced by finite difference approximations obtained via Taylor series at those discrete points. The aforementioned technique generates a large algebraic system of equations that needs to be solved, rather than the differential equation, which can be solved numerically on a computer.

Application of Finite Difference Method to TFKG Equation

The aim of this section is to develop a numerical scheme for the time fractional Klein-Gordon equation by applying the finite difference method. Before tackling the problem, we will employ the Crank-Nicolson finite difference approach to achieve more accurate results and to provide an implicit treatment of time, which yields:

$$\begin{aligned} D_t^\alpha u = &\frac{(u_{xx})^{n+1}+(u_{xx})^n}{2} + \frac{a}{2}(u^{n+1}+u^n) + \frac{b}{2}((u^2)^{n+1}+(u^2)^n) \\ &+\frac{c}{2}((u^3)^{n+1}+(u^3)^n) + \frac{g(x,t_{n+1})+g(x,t_n)}{2} \end{aligned} \tag{3}$$

Then, it is required to discretize the present problem in given computational and time domain. For this purpose, first of all we are going to use $L2$ algorithm to discretize time fractional derivative by using formula given as (Oldham & Spanier, 1974):

In order to discretize the problem in the given spatial and discrete time domain, we will first use the $L2$ algorithm. Specifically, we will employ the formula given by (Oldham & Spanier, 1974) for discretizing time fractional derivatives:

$$D_t^\alpha u = \frac{(\Delta t)^{-\alpha}}{\Gamma(3-\alpha)} \sum_{k=0}^{n-1} \omega_k^\alpha [u^{n-k} - 2u^{n-k-1} + u^{n-k-2}] \tag{4}$$

where $\omega_k^\alpha = \left(k+1\right)^{2-\alpha} - k^{2-\alpha}$. It is evident from (4) that the $L2$ algorithm has an implicit treatment of time. For the spatial derivative the term u_{xx}, a centered approximation for the second-order derivative is given as

$$u_{xx} = \frac{u_{j+1}-2u_j+u_{j-1}}{(\Delta x)^2} \tag{5}$$

As it seen from the equation given in $\left(3\right)$, $\left(u^2\right)^{n+1}$ and $\left(u^3\right)^{n+1}$ are nonlinear terms, so it is needed to linearize these terms by using Rubin Graves type linearization technique (Rubin & Graves, 1975):

$$\begin{aligned} (u^2)^{n+1} &= 2u^n u^{n+1} - (u^2)^n \\ (u^3)^{n+1} &= 3(u^n)^2 u^{n+1} - 2(u^3)^n. \end{aligned} \tag{6}$$

When we collect all finite difference approaches with $L2$ algorithm and Rubin Graves type linearization technique in $\left(3\right)$, we obtain the following algebraic equation

$$\begin{aligned} \frac{(\Delta t)^{-\alpha}}{\Gamma(3-\alpha)} \sum_{k=0}^{n-1} \omega_k^\alpha \left[u_j^{n-k} - 2u_j^{n-k-1} + u_j^{n-k-2}\right] = \left(\frac{u_{j+1}^{n+1}-2u_j^{n+1}+u_{j-1}^{n+1}}{2(\Delta x)^2} + \frac{u_{j+1}^n-2u_j^n+u_{j-1}^n}{2(\Delta x)^2}\right) \\ +\frac{a}{2}(u^{n+1}+u^n) + \frac{b}{2}\left(2u_j^n u_j^{n+1}\right) + \frac{c}{2}\left(3\left(u_j^n\right)^2 u^{n+1} - (u^3)^n\right) + \frac{g(x,t_{n+1})+g(x,t_n)}{2} \end{aligned} \tag{7}$$

After some arrangements, we get an algebraic equation system in the following form

$$u_{j-1}^{n+1}\left(-\frac{S}{2(\Delta x)^2}\right)+u_j^{n+1}\left(1+\frac{S}{(\Delta x)^2}-\frac{S}{2}\left(a+2b\left(u_j^n\right)+3c\left(u_j^n\right)^2\right)\right)+u_{j-1}^{n+1}\left(-\frac{S}{2(\Delta x)^2}\right)$$

$$=u_{j-1}^{n}\left(\frac{S}{2(\Delta x)^2}\right)+u_j^{n}\left(2-\frac{S}{(\Delta x)^2}+\frac{S}{2}\left(a-c\left(u_j^n\right)^2\right)\right)+u_{j-1}^{n}\left(\frac{S}{2(\Delta x)^2}\right) \tag{8}$$

$$-u_j^{n-1}+\frac{g(x,t_{n+1})+g(x,t_n)}{2}-\sum_{k=1}^{n}\omega_k^{\alpha}\left[u_j^{n+1-k}-2u_j^{n-k}+u_j^{n-k-1}\right],$$

where $S=(\Delta t)^{\alpha}\,\Gamma(3-\alpha)$. It can be seen from the (8), for $j=1,2,..,N$, u_0^{n+1} and u_0^{n} are boundaries, this values are known from boundary conditions $u(x_L,t)$ and $u(x_R,t)$ because of spatial domain discretization as $x_L=x_0$ and $x_L=x_N$. For $n=0,1,2,..,M$, the u_j^{n-1} function is out of time domain, when we use initial condition given in (2) with central difference approximation for first order derivative, we get $u_j^{n+1}=2\Delta t\ u_1(x)+u_j^{n-1}$. At the end of this section, one has an algebraic equation system in the form of (8). Solving the system iteratively results in obtaining the values of unknown function $u(x,t)$ at time nodes $(n+1)$ the using the known values of function $u(x,t)$ at the time level nodes (n) for every computational nodes. With a view to get an initial vector to begin iteration, the initial condition $u(x,0)=u_0(x)$ given in (2) for all values of computational domain nodes as $u(x_L,0)=u_0(x_L)$, $u(x_1,0)=u_0(x_1),\ldots,$ $u(x_{N-1},0)=u_0(x_{N-1})$, $u(x_R,0)=u_0(x_R)$.

Stability Analysis

In this section, we are going to investigate the stability analysis of the Crank-Nicolson scheme obtained for the time-dependent Klein-Gordon equation for the force-free case using von Neumann stability analysis. For this reason, we are going to look for the solutions in the following form:

$$u_j^n=\lambda^n e^{ijh\phi} \tag{9}$$

where $i=\sqrt{-1}$, ϕ is grid wave number and λ is growth factor. The goal is to obtain a condition for stability for $|\lambda|\le 1$. In order to achive our aim, let us consider linearized scheme for time fractional Klein Gordon equation as follows;

$$\frac{(\Delta t)^{-\alpha}}{\Gamma(3-\alpha)}\sum_{k=1}^{n}\omega_k^{\alpha}\left[u_j^{n+1-k}-2u_j^{n-k}+u_j^{n-k-1}\right]$$

$$-\left(\frac{u_{j+1}^{n+1}-2u_j^{n+1}+u_{j-1}^{n+1}}{2(\Delta x)^2}+\frac{u_{j+1}^{n}-2u_j^{n}+u_{j-1}^{n}}{2(\Delta x)^2}\right)-\frac{\hat{u}}{2}\left(u^{n+1}+u^{n}\right)=0 \tag{10}$$

when we use (9) in (10), it yields

$$\hat{S}_{\alpha,t}\sum_{k=1}^{n}\omega_k^{\alpha}e^{ijh\phi}\left(\lambda^{n+1-k}-2\lambda^{n-k}+\lambda^{n-1-k}\right)-\frac{1}{2(\Delta x)^2}\lambda^{n+1}e^{ijh\phi}(2\cos(h\phi)-2)$$

$$-\frac{1}{2(\Delta x)^2}\lambda^{n}e^{ijh\phi}(2\cos(h\phi)-2)-\frac{\hat{u}}{2}e^{ijh\phi}\left(\lambda^{n+1}+\lambda^{n}\right)=0 \tag{11}$$

where $\hat{u}$ is linearized term, $\hat{S}_{\alpha,t}=1/S$. For $n=0$ and after some arrangments, we get

$$\lambda^3\left\{\hat{S}_{\alpha,t}+2\sin^2\left(\frac{h\phi}{2}\right)-\hat{u}\right\}+\lambda^2\left\{-\hat{S}_{\alpha,t}+(2^{2-\alpha}-1)\hat{S}_{\alpha,t}+2\sin^2\left(\frac{h\phi}{2}\right)-\hat{u}\right\}$$

$$+\lambda\left\{\hat{S}_{\alpha,t}-2(2^{2-\alpha}-1)\hat{S}_{\alpha,t}\right\}+(2^{2-\alpha}-1)\hat{S}_{\alpha,t}=0 \tag{12}$$

if we express (12) more simply in polynomial form, it yields

$$\tilde{a}\,\lambda^3 + \tilde{b}\,\lambda^2 + \tilde{c}\,\lambda + \tilde{d} = 0 \tag{13}$$

Therefore, the roots of (13) can be obtained as

$$\lambda_1 = p_1 - p_2 + p_3$$
$$\lambda_2 = p_1 + \frac{1}{2}(1 + i\sqrt{3})p_2 - \frac{1}{2}(1 - i\sqrt{3})p_3$$
$$\lambda_3 = p_1 + \frac{1}{2}(1 - i\sqrt{3})p_2 - \frac{1}{2}(1 + i\sqrt{3})p_3$$

and

$$\begin{aligned}
|\lambda_1| &= \sqrt{(p_1 - p_2 + p_3)^2} \\
|\lambda_2| &= \sqrt{\left(p_1 + \tfrac{1}{2}(p_2 - p_3)^2\right) + \tfrac{\sqrt{3}}{2}(p_2 + p_3)^2} \\
|\lambda_3| &= \sqrt{\left(p_1 + \tfrac{1}{2}(p_2 - p_3)^2\right) + \tfrac{\sqrt{3}}{2}(p_2 + p_3)^2}
\end{aligned} \tag{14}$$

where

$$p_1 = -\frac{\tilde{b}}{3\,\tilde{a}}$$

$$p_2 = \frac{\sqrt[3]{2}\left(3\tilde{a}\tilde{c} - \tilde{b}^2\right)}{3\tilde{a}\sqrt[3]{\sqrt{\left(-27\tilde{a}^2\tilde{d} + 9\tilde{a}\tilde{b}\tilde{c} - 2\tilde{b}^3\right)^2 + 4\left(3\tilde{a}\tilde{c} - \tilde{b}^2\right)^3} - 27\tilde{a}^2\tilde{d} + 9\tilde{a}\tilde{b}\tilde{c} - 2\tilde{b}^3}}$$

$$p_3 = \frac{\sqrt[3]{\sqrt{\left(-27\tilde{a}^2\tilde{d} + 9\tilde{a}\tilde{b}\tilde{c} - 2\tilde{b}^3\right)^2 + 4\left(3\tilde{a}\tilde{c} - \tilde{b}^2\right)^3} - 27\tilde{a}^2\tilde{d} + 9\tilde{a}\tilde{b}\tilde{c} - 2\tilde{b}^3}}{3\sqrt[3]{2}\tilde{a}}$$

in order to obtain the values of roots, we are going to use the maximum values of variables and compute (14), The following table can be given,

Table 1. The values of the eigenvalues

Δx	Δt	α	ϕ	$\lvert\lambda_1\rvert$	$\lvert\lambda_2\rvert = \lvert\lambda_3\rvert$
0.5	0.5	2	π	5.55112×10^{-17}	0.565685
0.75	0.75	2	π	5.55112×10^{-17}	0.552052
1	1	2	π	1.11022×10^{-16}	0.541928

RESULTS AND DISCUSSION

In this section, we present numerical solutions to the time fractional Klein-Gordon equation for various temporal and spatial steps, as well as different values of the fractional order. We consider the equation given in (1), along with the specified initial and boundary conditions.

$$u(x_L, t) = u_L(t), \qquad u(x_R, t) = u_R(t), \quad t \geq 0$$
$$u(x, 0) = f_1(x), \qquad u_t(x, 0) = f_2(x), \quad a \leq x \leq b.$$

The error norms L_2 and L_∞ are calculated using following formulae

$$L_2 = \sum_{i=0}^{N} \sqrt{\left(\left(u(x_i,t)\right) - u_{num}(x_i,t)\right)^2}, (x,t) \in x_L, x_R] \times 0, T]$$
$$L_\infty = \max_{0 \le i \le N} |u(x_i,t) - u_{num}(x_i,t)|$$

Example 1:

For first example, we are going to consider time fractional Klein Gordon equation with the coohing the coefficients related with equation as $a = 0$, $b = -1$, and $c = 0$. And the domain of the mentioned problem is $x \in [0,1]$, $t \in [0,1]$. Thus equation and related boundary and initial conditions can be expressed as (Mulimani & Kumbinarasaiah, 2024)

$$\begin{aligned} &D_t^\alpha u = u_{xx} - u^2 + g(x,t) \\ &u(0,t) = 0,\ u(1,t) = t^3 \\ &u(x,0) = 0,\ u_t(x,0) = 0 \end{aligned} \tag{15}$$

The exact solution of the problem is $u(x,t) = x^3 t^3$ and forced term is $g(x,t) = -6xt^3 + x^6t^6 + \frac{6x^3t^{3-\alpha}}{\Gamma(4-\alpha)}$. First of all, we present the change of error norms for different times while a changing to $\alpha = 1.2$, $1.5, 1.75$. For table 2, the partition of computational domain is $N = 40$, and time domain is $M = 1000$. It is clear from Table 2, for all selected values of fractional order, error norms remain relatively small. Additionally, for $\alpha = 1.2$, the error norms is L_2 =1.6699362×10^{-8} and L_∞ =2.8115151×10^{-8} while L_2 =6.6920342×10^{-8} and L_∞ =9.8143084×10^{-8} at=0.1. The behavior of numerical solutions is an expected outcome when considering rounding errors.

Table 2. The error norms for different values of fractional order α for Example 1

	$\alpha = 1.2$		$\alpha = 1.5$		$\alpha = 1.75$	
t	L_2	L_∞	L_2	L_∞	L_2	L_∞
0.1	1.6699362×10^{-8}	2.8115151×10^{-8}	2.2764702×10^{-7}	4.3462997×10^{-7}	1.1511139×10^{-6}	2.4407432×10^{-6}
0.2	2.9596141×10^{-8}	4.4956871×10^{-8}	4.8768308×10^{-7}	8.1901650×10^{-7}	3.0962677×10^{-6}	5.8108280×10^{-6}
0.3	3.7841647×10^{-8}	5.5218544×10^{-8}	7.0328424×10^{-7}	1.0811117×10^{-7}	5.0829910×10^{-6}	8.6537974×10^{-6}
0.4	4.2596202×10^{-8}	6.1342199×10^{-8}	8.6862129×10^{-7}	1.2602275×10^{-6}	6.8879808×10^{-6}	1.0825292×10^{-5}
0.5	4.5334159×10^{-8}	6.5025259×10^{-8}	9.7677852×10^{-7}	1.3793153×10^{-6}	8.4412827×10^{-6}	1.2410636×10^{-5}
0.6	4.7393399×10^{-8}	6.8002836×10^{-8}	1.0269751×10^{-6}	1.4406220×10^{-6}	9.6722860×10^{-6}	1.3543809×10^{-5}
0.7	4.9821272×10^{-8}	7.1655979×10^{-8}	1.0288348×10^{-6}	1.4456171×10^{-6}	1.0465453×10^{-5}	1.4293328×10^{-5}
0.8	5.3435812×10^{-8}	7.7226694×10^{-8}	9.9774066×10^{-7}	1.4071806×10^{-6}	1.0736118×10^{-5}	1.4630022×10^{-5}
0.9	5.8925206×10^{-8}	8.5720178×10^{-8}	9.5013279×10^{-7}	1.3457568×10^{-6}	1.0501671×10^{-5}	1.4483051×10^{-5}
1	6.6920342×10^{-8}	9.8143084×10^{-8}	9.0021308×10^{-7}	1.2798797×10^{-6}	9.8520061×10^{-6}	1.3800674×10^{-5}

The comparison results with (Mulimani & Kumbinarasaiah, 2024) is presented in Table 3 for the values of $t = 0.01$ and 0.001 at different nodes of computation domain. In (Mulimani & Kumbinarasaiah, 2024), the authors used Fibonacci wavelets for solving the equation and they constructed the operational matrices of integration. To be able to match the nodal points of the compared studies, the partition of the space and time domains are selected as $N = 10, M = 1000$, thus, in Table 3, a comparison table is obtained and presented for $\alpha = 2$. It is obvious from the table, for the point $x = 0.1$, the absolute error is 3.6386×10^{-8} for (Mulimani & Kumbinarasaiah, 2024) and $1.4079950 \times 10^{-10}$ for present method, however, for the point $x = 0.5$, the absolute error is 1.6168×10^{-8} for (Mulimani & Kumbinarasaiah, 2024) and 1.7503997×10^{-8} for present method for $t = 0.01$. For $t = 0.001$, It can be say the results obtained from Crank-Nicolson finite difference method gives more accurate results than those in (Mulimani & Kumbinarasaiah, 2024) . In general, the results obtained using the Crank-Nicolson finite difference method has an aggrement with those of (Mulimani & Kumbinarasaiah, 2024) and have yielded more accurate in most of the selected points.

Table 3. A comparison between absolute errors at different points for Example 1

	t=0.01		t=0.001	
x	(Mulimani & Kumbinarasaiah, 2024)	present	(Mulimani & Kumbinarasaiah, 2024)	present
0.1	3.6386×10^{-8}	$1.4079950 \times 10^{-10}$	3.6386×10^{-10}	$5.0007500 \times 10^{-13}$
0.2	7.1872×10^{-8}	1.1215990×10^{-9}	7.1872×10^{-10}	$4.0001500 \times 10^{-12}$
0.3	1.0546×10^{-8}	3.7823985×10^{-9}	1.0546×10^{-10}	$1.3500225 \times 10^{-11}$
0.4	1.3594×10^{-8}	8.9631980×10^{-9}	1.3594×10^{-10}	$3.2000300 \times 10^{-11}$
0.5	1.6168×10^{-8}	1.7503997×10^{-8}	1.6168×10^{-10}	$6.2500375 \times 10^{-11}$
0.6	1.8035×10^{-8}	3.0244797×10^{-8}	1.8035×10^{-10}	$1.0800045 \times 10^{-10}$
0.7	1.8830×10^{-8}	4.8025596×10^{-8}	1.8830×10^{-9}	$1.7150052 \times 10^{-10}$
0.8	1.7929×10^{-7}	7.1686334×10^{-8}	1.7929×10^{-9}	$2.5600060 \times 10^{-10}$
0.9	1.4131×10^{-7}	$1.01934065 \times 10^{-7}$	1.4131×10^{-9}	$3.6448817 \times 10^{-10}$

Lastly, the numerical behaviour of the problem is displayed in Figures 1-3. Figure 1 shows the change of the graph with the change of the fractional order derivative values α for $N = 100$ and $M = 20$. Figure 2 includes the numerical behaviour of solutions at different time levels. and Figure 3 provides a three-dimensional view of the numerical solutions.

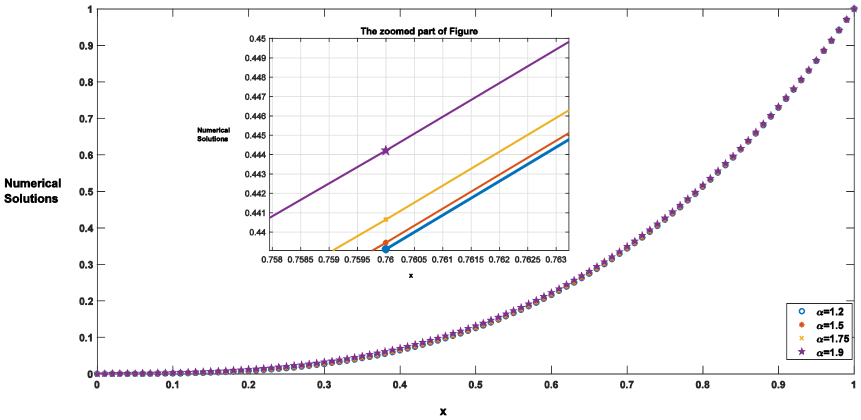

Figure 1. The numerical behaviour of time fractional Klein Gordon equation for different values of α for example 1

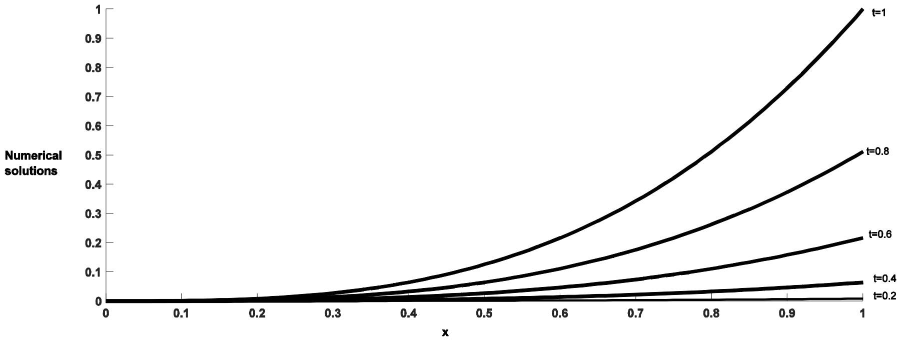

Figure 2. The numerical behaviour of time fractional Klein Gordon equation at different time levels for example 1

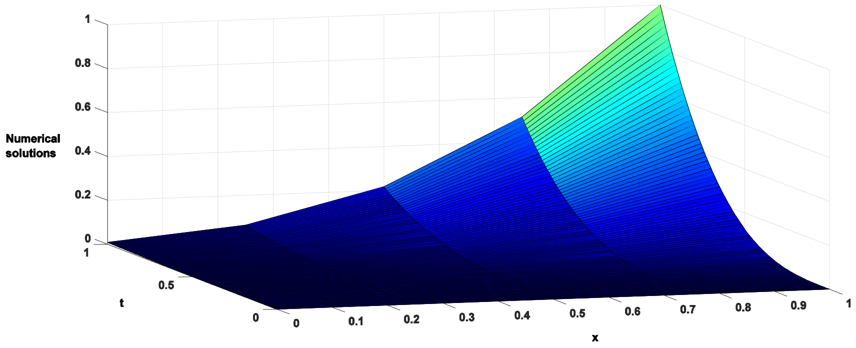

Figure 3. The 3 dimensional graph of time fractional Klein Gordon equation for example 1

Example 2:

As the second example, consider time fractional Klein Gordon equation in (1) with related coefficients $a=-1,\ b=0,$ and $c=-3/2.$ Thus, the equation can be rewritten as follows (Nagy, 2017)

$$D_t^{\alpha}u = u_{xx} - u - \frac{3}{2}cu^3 + g(x,t) \tag{16}$$

$$\begin{aligned} &u(x_L,t)=u_L(t), \quad u(x_R,t)=u_R(t), \quad x_L \le x \le x_R \\ &u(x,0)=f_1(x), \quad\ \ u_t(x,0)=f_2(x), \quad\ \ 0 \le t \le T. \end{aligned} \tag{17}$$

where $u_L(t)=u_R(t)=0\ and\ f_1(x)=f_2(x)=0$. The exact solution and forced term of the problem given in $(16)-(17)$ are :

$$u(x,t)=\sin(\pi x)t^{2+\alpha}$$

$$\begin{aligned} g(x,t) &= \frac{1}{2}\Gamma(3+\alpha)\sin(\pi x)t^2 + (1+\pi^2)t^{2+\alpha}\sin(\pi x) \\ &+\frac{3}{2}(\sin(\pi x)t^{2+\alpha})^3. \end{aligned} \tag{18}$$

The initial and boundary conditions of the problem are taken from the exact solution $u(x,t)$ given in Eq. (18). As in the first example, the domain of the problem is chosen to be $(x,t)=[0,1]\times[0,1]$ and the Table 3 presents values of error norms for different values of the fractional order α. Thus, when the Table 4 is analysed, it is found that the error norms were quite small. The finite difference method's characteristic structure allows it to be applied directly to the problem, and it uses Taylor series expansions of derivatives. The method's focus on nodal points highlights their critical role in determining the accuracy of the solution. While the method can be applied directly to many problems, its application can be challenging in complex geometries or irregular areas, where irregular boundaries and curved shapes can lead to inaccurate results. The method relies on finite difference approximations, which reveals truncation errors due to its nature. These errors can impact the accuracy of the solution, which depends on two key factors: grid spacing and the order of the finite difference scheme used. A finer grid spacing or higher-order scheme can improve accuracy, but also increases computational cost.

For the second problem, Table 4-9 are prepared. In Table 4, N=40 and M=1000 are chosen, and the error norms for different values of the fractional order derivative are presented. Similar to the previous example, it is observed that the error norms for the selected values of the fractional order derivative were quite small. In Table 5, a comparison of absolute errors with (Nagy, 2017) at some selected nodal points x at t=1 is presented for fractional order derivatives values $\alpha=$ 1.5, 1.7, and 1.9. Again, to enable the matching of nodal points, N=100 and M=1000 are selected. It is clearly evident from the table that the numerical results obtained using the Crank-Nicolson finite difference method have shown more accurate results than those generated by the shifted Chebyshev polynomial method employed in Nagy's study.

Table 4. The error norms for different values of fractional order α for example 2

	$\alpha=1.2$		$\alpha=1.5$		$\alpha=1.75$	
t	L_2	L_∞	L_2	L_∞	L_2	L_∞
0.1	8.3937230×10^{-8}	1.1870516×10^{-7}	2.8787591×10^{-7}	4.0711801×10^{-7}	6.8841173×10^{-7}	9.7356121×10^{-7}
0.2	5.6331068×10^{-7}	7.9664162×10^{-7}	1.1337769×10^{-6}	1.6034026×10^{-6}	3.7582122×10^{-6}	5.3149146×10^{-6}
0.3	2.4895541×10^{-6}	3.5207545×10^{-6}	2.7828012×10^{-6}	3.9354728×10^{-6}	9.9136782×10^{-6}	1.4020055×10^{-5}
0.4	7.5546960×10^{-6}	1.0683754×10^{-5}	6.0925817×10^{-6}	8.6161554×10^{-6}	1.9515590×10^{-5}	2.7599139×10^{-5}
0.5	1.7851090×10^{-6}	2.5242882×10^{-5}	1.2674943×10^{-5}	1.7924372×10^{-5}	3.3060012×10^{-5}	4.6753009×10^{-5}
0.6	3.5662684×10^{-6}	5.0417743×10^{-5}	2.4887627×10^{-5}	3.5190542×10^{-5}	5.1558013×10^{-5}	7.2907074×10^{-5}
0.7	6.3192839×10^{-5}	8.9282224×10^{-5}	4.5688768×10^{-5}	6.4577551×10^{-5}	7.6804861×10^{-5}	1.0857963×10^{-4}
0.8	1.0200926×10^{-4}	1.4392132×10^{-4}	7.8277835×10^{-4}	1.1052745×10^{-4}	1.1143611×10^{-4}	1.5742114×10^{-4}
0.9	1.5188041×10^{-4}	2.1367426×10^{-4}	1.2524567×10^{-4}	1.7643678×10^{-4}	1.5854430×10^{-4}	2.2355972×10^{-4}
1	2.0881410×10^{-4}	2.9222268×10^{-4}	1.8665723×10^{-4}	2.6169098×10^{-4}	2.2035734×10^{-4}	3.0945840×10^{-4}

Table 5. A comparison between absolute errors at different points for example 2

	$\alpha=1.5$		$\alpha=1.7$		$\alpha=1.9$	
t	SCCM (Nagy, 2017)	Present	SCCM (Nagy, 2017)	Present	SCCM (Nagy, 2017)	Present
0.1	1.6396×10^{-3}	1.5708654×10^{-5}	1.5471×10^{-3}	3.2132612×10^{-5}	1.4380×10^{-3}	1.5419438×10^{-4}
0.2	1.2808×10^{-3}	2.9647016×10^{-5}	1.1272×10^{-3}	6.0651171×10^{-5}	9.4914×10^{-4}	2.9137763×10^{-4}
0.3	1.0869×10^{-3}	4.0412908×10^{-5}	8.9663×10^{-4}	8.2687099×10^{-5}	6.7913×10^{-4}	3.9780051×10^{-4}
0.4	8.4196×10^{-4}	4.7137617×10^{-5}	6.3348×10^{-4}	9.6456226×10^{-5}	3.9687×10^{-4}	4.6457012×10^{-4}
0.5	7.8252×10^{-4}	4.9415292×10^{-5}	5.6868×10^{-4}	1.0112079×10^{-4}	3.2651×10^{-4}	4.8724770×10^{-4}
0.6	8.4196×10^{-4}	4.7137617×10^{-5}	6.3348×10^{-4}	9.6456226×10^{-5}	3.9687×10^{-4}	4.6457012×10^{-4}
0.7	1.0869×10^{-3}	4.0412908×10^{-5}	8.9663×10^{-4}	8.2687099×10^{-5}	6.7913×10^{-4}	3.9780051×10^{-4}
0.8	1.2808×10^{-3}	2.9647016×10^{-5}	1.1272×10^{-3}	6.0651171×10^{-5}	9.4914×10^{-4}	2.9137763×10^{-4}
0.9	1.6396×10^{-3}	1.5708654×10^{-5}	1.5471×10^{-3}	3.2132612×10^{-5}	1.4380×10^{-3}	1.54194387×10^{-4}
L_2		3.52187482×10^{-5}		7.20621073×10^{-5}		3.46829249×10^{-4}
L_∞		4.94152920×10^{-5}		1.01120790×10^{-4}		4.87247702×10^{-4}

Tables 6 and 7 contain a comparison of the fractional order derivatives at values 1.4 and 1.6 for (Odibat & Momani, 2009), (Nagy, 2017), (Amin et al., 2020), and (Sahu & Jena, 2024). To ensure the matching of the nodes, N=100, M=1000, and t=1 have been chosen. The presented tables serve as a comparison of absolute error norms. It is observed from the tables that the results obtained with the presented method are more accurate at the selected points compared to (Odibat & Momani, 2009), (Nagy, 2017), (Amin et al., 2020), and show more accurate results than (Sahu & Jena, 2024 at the majority of the selected points. Overall, it can be noted that the absolute errors are consistent. Finally, a comparison of absolute error norms with (Yaseen et al., 2021) and (Vivas-Cortez et al., 2024) is presented in Tables 8-9 for N=100 and M=1000. It can be observed that for the fractional derivative $\alpha=1.5$, the Crank-Nicolson finite difference method yields more accurate results. For a fractional derivative $\alpha=1.7$, more accurate results are achieved compared to (Yaseen et al., 2021), and the results have a closely agreement with those from (Vivas-Cortez et al., 2024).

Table 6. A comparison between absolute errors at different points for example 2

$\alpha = 1.4$					
x	VIM (Odibat & Momani, 2009)	(Amin et al., 2020)	SCCM (Nagy, 2017)	(Sahu & Jena, 2024)	Present
(0.1, 0.1)	3.9211×10^{-5}	1.9749×10^{-6}	2.3809×10^{-5}	5.84378×10^{-9}	8.1986800×10^{-8}
(0.2,0.2)	6.1713×10^{-4}	1.7326×10^{-5}	5.2644×10^{-5}	2.15662×10^{-6}	4.9378183×10^{-7}
(0.3,0.3)	2.1989×10^{-3}	5.2839×10^{-6}	6.0187×10^{-6}	6.47028×10^{-5}	1.3377750×10^{-6}
(0.4,0.4)	2.5545×10^{-3}	9.9062×10^{-6}	6.6640×10^{-5}	6.77903×10^{-4}	2.7391374×10^{-6}
(0.5,0.5)	5.3405×10^{-3}	1.3396×10^{-6}	4.0011×10^{-5}	3.89735×10^{-3}	4.9096307×10^{-6}
(0.6,0.6)	3.1409×10^{-2}	1.3557×10^{-5}	1.5837×10^{-4}	1.48996×10^{-2}	7.8937858×10^{-6}
(0.7,0.7)	8.0092×10^{-2}	9.6832×10^{-6}	9.1922×10^{-4}	4.10203×10^{-2}	1.1095407×10^{-5}
(0.8,0.8)	1.3528×10^{-1}	3.5290×10^{-5}	2.9084×10^{-3}	8.04521×10^{-2}	1.2841522×10^{-5}
(0.9,0.9)	1.4272×10^{-1}	9.0059×10^{-6}	3.8732×10^{-3}	9.42919×10^{-2}	1.0287723×10^{-5}

Table 7. A comparison between absolute errors at different points for example 2

$\alpha = 1.6$					
x	VIM (Odibat & Momani, 2009)	(Amin et al., 2020)	SCCM (Nagy, 2017)	(Sahu & Jena, 2024)	Present
(0.1, 0.1)	1.0402×10^{-5}	1.4963×10^{-6}	2.3809×10^{-5}	2.20655×10^{-10}	1.8140413×10^{-7}
(0.2,0.2)	1.4424×10^{-4}	1.5765×10^{-6}	5.2644×10^{-5}	1.41787×10^{-7}	1.4830111×10^{-6}
(0.3,0.3)	6.7115×10^{-5}	2.1699×10^{-7}	6.0187×10^{-6}	5.88593×10^{-6}	4.5728868×10^{-6}
(0.4,0.4)	3.0493×10^{-3}	1.1769×10^{-6}	6.4440×10^{-5}	7.77198×10^{-5}	9.2450831×10^{-6}
(0.5,0.5)	1.6350×10^{-2}	1.2375×10^{-6}	4.0011×10^{-5}	5.35285×10^{-4}	1.4599743×10^{-5}
(0.6,0.6)	4.9599×10^{-2}	2.1232×10^{-6}	1.5837×10^{-4}	2.37362×10^{-3}	1.9403104×10^{-5}
(0.7,0.7)	1.0675×10^{-1}	1.8721×10^{-6}	9.1922×10^{-4}	7.42466×10^{-3}	2.2265420×10^{-5}
(0.8,0.8)	1.6942×10^{-1}	1.0951×10^{-5}	2.9084×10^{-3}	1.64614×10^{-2}	2.1522751×10^{-5}
(0.9,0.9)	1.7521×10^{-1}	2.2989×10^{-5}	3.8732×10^{-3}	2.2289×10^{-2}	1.4986281×10^{-5}

Table 8. A comparison between absolute errors at different nodal points for example 2

$\alpha = 1.5$			
x	(Yaseen et al., 2021)	(Vivas-Cortez et al., 2024)	Present
0.1	2.2437×10^{-4}	3.7667×10^{-5}	1.57086543×10^{-5}
0.2	4.4180×10^{-4}	7.0999×10^{-5}	2.96470163×10^{-5}
0.3	6.3346×10^{-4}	9.6627×10^{-5}	4.04129089×10^{-5}
0.4	7.6861×10^{-4}	1.1255×10^{-4}	4.71376174×10^{-5}
0.5	8.1773×10^{-4}	1.1793×10^{-4}	4.94152920×10^{-5}
0.6	7.6861×10^{-4}	1.1255×10^{-4}	4.71376175×10^{-5}
0.7	6.3346×10^{-4}	9.6627×10^{-5}	4.04129089×10^{-5}
0.8	4.4180×10^{-4}	7.0999×10^{-5}	2.96470163×10^{-5}
0.9	2.2437×10^{-4}	3.7667×10^{-5}	1.57086543×10^{-5}

Table 9. A comparison between absolute errors at different nodal points for example 2

$\alpha = 1.7$			
x	(Yaseen et al., 2021)	(Vivas-Cortez et al., 2024)	Present
0.1	2.8566×10^{-4}	1.2052×10^{-5}	3.21326128×10^{-5}
0.2	5.5578×10^{-4}	2.2820×10^{-5}	6.06511717×10^{-5}
0.3	7.8594×10^{-4}	3.1232×10^{-5}	8.26870994×10^{-5}
0.4	9.4376×10^{-4}	3.6548×10^{-5}	9.64562265×10^{-5}
0.5	1.0003×10^{-3}	3.8361×10^{-5}	1.01120790×10^{-4}
0.6	9.4376×10^{-4}	3.6548×10^{-5}	9.64562265×10^{-5}

Table 9. A comparison between absolute errors at different nodal points for example 2 (Continued)

x	(Yaseen et al., 2021)	(Vivas-Cortez et al., 2024)	Present
0.7	7.8594×10^{-4}	3.1232×10^{-5}	7.68842122×10^{-5}
0.8	5.5578×10^{-4}	2.2820×10^{-5}	6.06511717×10^{-5}
0.9	2.8566×10^{-4}	1.2052×10^{-5}	3.21326128×10^{-5}

The simulations of the numerical solutions are depicted in Figures 4-6. The first of figures includes the behaviour of solutions for different fractional order while second figure shows behaviour at different time levels. At the end figure involves 3 dimensional aspect of the numerical solutions.

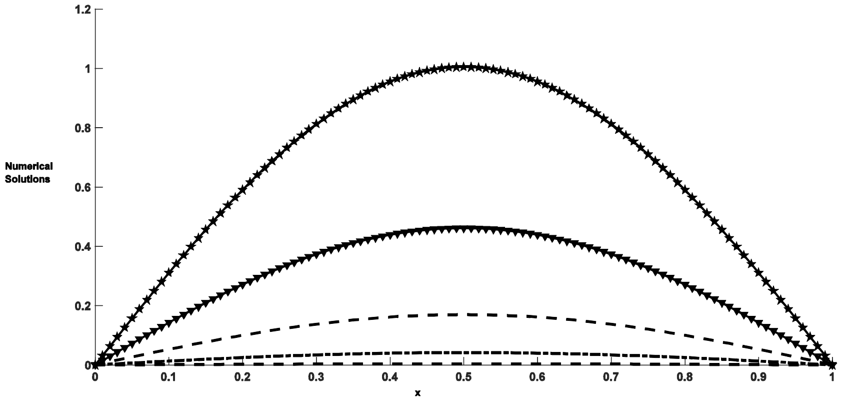

Figure 4. The numerical behaviour of time fractional Klein Gordon equation for different values of α for example 2

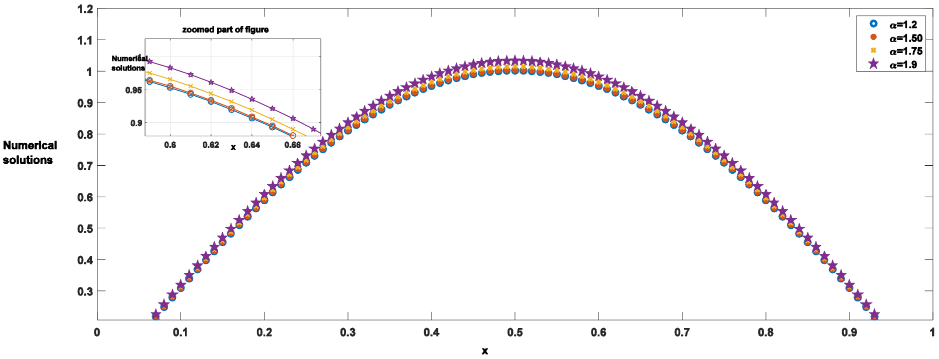

Figure 5. The numerical behaviour of time fractional Klein Gordon equation at different time levels for example 2

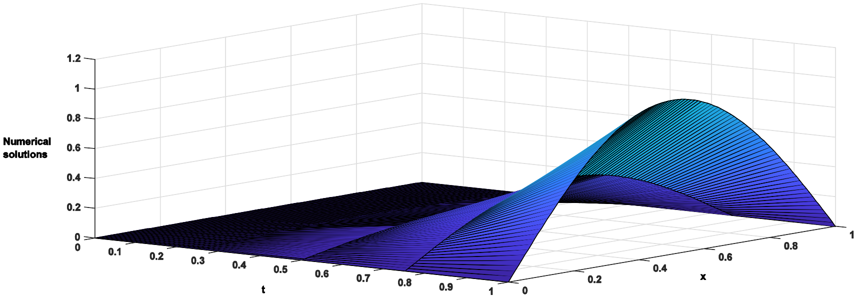

Figure 6: The 3 dimensional graph of time fractional Klein Gordon equation for example 2

It is essential to emphasize that the fractional Klein-Gordon equation is used to model various physical phenomena. Therefore, solutions of this equation have significant physical importance in various fields. For instance, it describes anomalous diffusion and wave propagation in quantum fields, extends the application of standard quantum theories to real-world phenomena, and describes the behavior of particles and quasiparticles in complex disordered systems. Solving the equation provides valuable insights into these systems, enabling predictions and a deeper understanding for field researchers in the daily applications of their experiments.

CONCLUSION

As a conclusion, in this paper, a Crank-Nicolson finite difference method is applied to obtain numerical solutions of the fractional order Klein Gordon equation. The $L2$ algorithm and the Crank-Nicolson approach are used for the discretization of the considered equation with respect to temporal variable, while central finite difference approaches are used for the discretization with respect to spatial variable. The fractional order equation is transformed into a system of algebraic equations and thus numerical solutions are obtained. The absolute error norms at the points and the error norms L_2 and L_∞ for different time, space steps and fractional orders are presented for the two problems related to the equation. If one considers the obtained results , it is observed that the Crank-Nicolson finite difference method is an effective and powerful method. The method can be considered as one of the best and applicable alternative ways to solve the nonlinear differential equations. Additionally, in future studies different techniques based on finite difference approach can be combined with variety of linearization technique and algorithm for discretization of fractional derivative can be applied such nonlinear problems arise in mathematics and physics.

Conflict of Interest

The article authors declare that there is no conflict of interest between them.

Author’s Contributions

The authors declare that they have contributed equally to the article.

REFERENCES

Akram, T., Abbas, M., Riaz, M. B., Ismail, A. I. and Ali, N. M. (2020). Development and analysis of new approximation of extended cubic b-spline to the nonlinear time fractional klein–gordon equation. *Fractals,* 28(08) , 2040039.

Amin, M., Abbas, M., Iqbal, M. K., Baleanu, D.(2020). Numerical treatment of time-fractional Klein–Gordon equation using redefined extended cubic B-spline functions. *Frontiers in Physic,* 8, 288.

Bansu, H., Kumar, S.(2021). Numerical solution of space-time fractional Klein-Gordon equation by radial basis functions and Chebyshev polynomials. *International Journal of Applied and Computational Mathematics,* 7, 1-19.

Biswas B, (2024). Analytical Solutions of the D-dimensional Klein-Gordon equation with q-deformed modified Pöschl-Teller Potential. *Electronic Journal of Applied Mathematics,* 2,1,14-21.

Dehghan, M., Abbaszadeh, M. and Mohebbi, A. (2015). An implicit RBF meshless approach for solving the time fractional nonlinear sine-Gordon and Klein–Gordon equations. *Engineering Analysis with Boundary Elements,* 50, 412-434.

Ganji, R. M., Jafari, H., Kgarose, M. and Mohammadi, A. (2021). Numerical solutions of time-fractional Klein-Gordon equations by clique polynomials. *Alexandria Engineering Journal* , 60.5, 4563-4571.

Habjia, A., Hajaji, A. E., Ghordaf, J. E., Hilal, K., & Charhabil, A. (2024). High-Precision Method for Space-Time-Fractional Klein-Gordon Equation. In *Applied Mathematics and Modelling in Finance, Marketing and Economics,* 1-14. Cham: Springer Nature Switzerland

Hashemizadeh, E., Ebrahimzadeh, A. (2018). An efficient numerical scheme to solve fractional diffusion-wave and fractional Klein–Gordon equations in fluid mechanics. *Physica A: Statistical Mechanics and its Applications,* 503, 1189-1203.

Korichi, Z., Souigat, A., Bekhouche, R., and Meftah, M. T. (2024). Solution of the fractional Liouville equation by using Riemann–Liouville and Caputo derivatives in statistical mechanics. *Theoretical and Mathematical Physics*, 218 (2), 336-345.

Mirzaei, S., & Shokri, A. (2024). Numerical study of the non-linear time fractional Klein-Gordon equation using the Pseudo-spectral Method. *Computational Methods for Differential Equations*.

Mulimani, M., Kumbinarasaiah, S.(2024). A numerical study on the nonlinear fractional Klein–Gordon equation. *Journal of Umm Al-Qura University for Applied Sciences* , 10.1, 178-199.

Mohebbi, A., Abbaszadeh, M., Dehghan, M. (2014). High-order difference scheme for the solution of linear time fractional Klein–Gordon equations. *Numerical Methods for Partial Differential Equations,* 30.4,1234-1253.

Nagy, A. M. (2017). Numerical solution of time fractional nonlinear Klein–Gordon equation using Sinc–Chebyshev collocation method, *Applied Mathematics and Computation.* 310 ,139-148.

Odibat, Z., Momani, S.(2009). The variational iteration method: an efficient scheme for handling fractional partial differential equations in fluid mechanics. *Comput Math Appl*., 58,2199–208.

Odibat, Z. (2024). Numerical simulation for an initial-boundary value problem of time-fractional Klein-Gordon equations. *Applied Numerical Mathematics*

Oldham, K., and Spanier, J. (1974). The fractional calculus theory and applications of differentiation and integration to arbitrary order. *Elsevier.*

Paredes, G. E. (2020). *Fractional-order models for nuclear reactor analysis*. Woodhead Publishing.

Rubin, S. G., Graves, R. A.(1975). *A cubic spline approximation for problems in fluid mechanics, National aeronauticsand space administration*. *Technical Report*, Washington, 1975.

Sahu, I., & Jena, S. R. (2024). An efficient technique for time fractional Klein-Gordon equation based on modified Laplace Adomian decomposition technique via hybridized Newton-Raphson Scheme arises in relativistic fractional quantum mechanics. *Partial Differential Equations in Applied Mathematics*, 100744.

Vivas-Cortez, M., Huntul, M. J., Khalid, M., Shafiq, M., Abbas, M., & Iqbal, M. K. (2024). Application of an Extended Cubic B-Spline to Find the Numerical Solution of the Generalized Nonlinear Time-Fractional Klein–Gordon Equation in Mathematical Physics. *Computation*, *12*(4), 80.

Yaseen M, Abbas M, Ahmad B(2021), Numerical simulation of the nonlinear generalized time-fractional Klein–Gordon equation using cubic trigonometric B-spline functions, *Mathematical Methods in the Applied Sciences* 44.1: 901-916.